

XUEBANG WU\*<sup>#</sup>, CHANGSONG LIU\***MECHANICAL SPECTROSCOPY: SOME APPLICATIONS ON STRUCTURAL CHANGES AND RELAXATION DYNAMICS IN SOFT MATTER****SPEKTROSKOPIA MECHANICZNA: NIEKTÓRE ZASTOSOWANIA DO ZMIAN STRUKTURALNYCH I DYNAMIKI RELAKSACJI W MATERII MIĘKKIEJ**

The general trend in soft matter is to study systems of increasing complexity covering a wide range in time and frequency. Mechanical spectroscopy is a powerful tool for understanding the structure and relaxation dynamics of these materials over a large temperature range and frequency scale. In this work, we collect a few recent applications using low-frequency mechanical spectroscopy for elucidating the structural changes and relaxation dynamics in soft matter, largely based on the author's group. We illustrate the potential of mechanical spectroscopy with three kinds of soft materials: colloids, polymers and granular systems. Examples include structural changes in colloids, segmental relaxations in amorphous polymers, and resonant dissipation of grain chains in three-dimensional media. The present work shows that mechanical spectroscopy has been applied as a necessary and complementary tool to study the dynamics of such complex systems.

*Keywords:* Polymer segmental dynamics, colloids, granular matter, mechanical spectroscopy

Ogólnym trendem w miękkiej materii jest, aby badać układy o rosnącej złożoności, obejmującej szeroki zakres czasu i częstotliwości. Spektroskopia mechaniczna jest potężnym narzędziem dla zrozumienia struktury i dynamiki relaksacji tych materiałów w szerokim zakresie temperatury i skali częstotliwości. W niniejszej pracy, zebraliśmy kilka ostatnich zastosowań spektroskopii mechanicznej niskiej częstotliwości do poznania zmian strukturalnych i dynamiki relaksacji w miękkiej materii, w dużej mierze opartych na grupie autorów. Opisujemy potencjał spektroskopii mechanicznej w przypadku trzech rodzajów materiałów miękkich: koloidów, polimerów i układów ziarnistych. Przykłady obejmują zmiany strukturalne w koloidach, segmentowe relaksacje amorficznych polimerów, i rezonansowe rozpraszanie łańcuchów ziaren w mediach trójwymiarowych. Niniejsza praca pokazuje, że spektroskopię mechaniczną zastosowano jako niezbędne i uzupełniające narzędzie do badania dynamiki takich systemów złożonych.

**1. Introduction**

Mechanical spectroscopy is a powerful tool for the investigations of crystal lattice defects (point defect, dislocations, grain boundary, etc.) and phase transformations in crystalline solids [1]. However, in the early 1990's the concept of soft matter has been proposed and the study of mechanical behaviors of these materials such as liquid crystals, granular matter, colloids and polymers poses a new challenge to the mechanical spectroscopy technique. Since then, the capabilities of traditional instruments such as inverted torsion pendulum have been improved to make it suitable and sensitive for dynamic relaxations and structural changes of liquids and soft matters. With an improved internal friction apparatus based on the traditional inverted torsion pendulum, the structural changes in liquid binary alloys, such as Pb-Sn, In-Sn, In-Bi, and As-Te have been studied, showing that mechanical spectroscopy is sensitive to liquid-liquid transition in binary alloys [2]. In

a general review, Cantelli systematically described the origin of the mechanical spectroscopy, its evolution, and its application in biological matter [3]. Since mechanical spectroscopy techniques cover timescales in the range about  $10^{-10}$ - $10^2$  s. This allows the study of different dynamical processes, from fast modes such as vibration and diffusion of atoms in solids, to slower modes including segmental relaxations and diffusion in polymers. And so considerable works about using mechanical spectroscopy have been found to study dynamics and phase transitions in soft and complex matter, such as polymers, granular matters and biological matters.

In this review, we do not present an exhaustive review on the different applications of mechanical spectroscopy to soft materials, but will focus on more specific phenomena, covering polymers, colloids, and granular matter, to demonstrate its versatility and effectiveness. We will start with recent advancements in mechanical spectroscopy instrumentation based on the inverted torsion pendulum, which

\* KEY LABORATORY OF MATERIALS PHYSICS, INSTITUTE OF SOLID STATE PHYSICS, CHINESE ACADEMY OF SCIENCES, P.O. BOX 1129, HEFEI, ANHUI, 230031, P.R. CHINA

<sup>#</sup> Corresponding author: xbwu@issp.ac.cn

make mechanical spectroscopy more relevant to soft matter research. The mechanical spectroscopy applications in areas such as phase behaviors in colloids, segmental relaxations in amorphous polymers, and resonant dissipation of grain matter will be discussed. We demonstrate that mechanical spectroscopy has been applied as a necessary and complementary tool in combination with other techniques in the studies of soft matter.

## 2. Mechanical spectroscopy technique

Mechanical spectroscopy measurements of the samples were made by using a modified low-frequency inverted torsion pendulum with a Couette-like setup using the forced-vibration method [4]. The apparatus proposed consists of the traditional torsion shaft equipped with two coaxial cylindrical cells for soft materials, as schematically in Fig. 1. Briefly, the operation of this apparatus is as follows: when the inner cylinder is immersed into the sample, an equal but opposite torque offered by a couple of electromagnets turns the torsion pendulum a small angle and is released. Unless the sample is extremely highly damped, the torsion pendulum system will oscillate, generating an oscillating shear flow of the sample with axial symmetry. Thus the mechanical loss of the sample can be determined. In the measurements, the inner cylinder is forced into torsional vibration by a time-dependent force  $F(t)=F_0\sin(\omega t)$ . The angular displacement function of the cylinder,  $A(t)$ , is measured optically. In the case here, the response of the argument  $A(t)=A_0\sin(\omega t-\varphi)$ , where  $\delta$  is the phase difference between  $F(t)$  and  $A(t)$ . The mechanical loss of the oscillating system, characterized by  $Q^{-1}$ , is given by

$$Q^{-1} = \frac{1}{2\pi} \frac{\Delta W}{W} = \frac{1}{2\pi} \frac{\int_0^{2\pi} F dA}{\int_0^{2\pi} dW - \frac{1}{4} \Delta W} = \frac{1}{2\pi} \frac{F_0 A_0 \pi \sin \varphi}{\frac{1}{2} F_0 A_0 \cos \varphi} = \tan \varphi, \quad (1)$$

where  $\Delta W$  and  $W$  are the dissipated energy and the maximum stored energy per cycle, respectively. In the measurement, the mechanical loss  $Q^{-1}$  and the relative modulus  $G$  ( $=F_0/A_0$ ) are measured as a function of temperature or frequency.

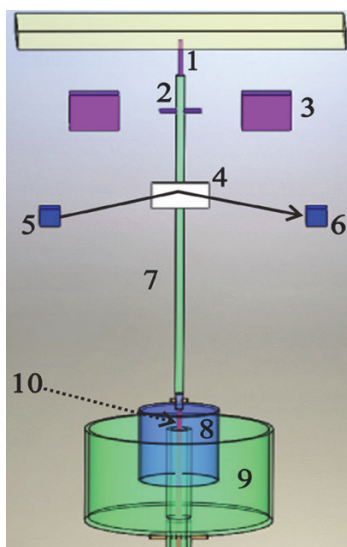


Fig. 1. Schematic diagram of the apparatus: 1, suspension wire; 2, permanent magnet; 3, external coils; 4, mirror; 5, light source; 6, photoreceiver; 7, pendulum rod; 8, inner cup; 9, outer cup; 10, torsion spring wire

## 3. Example Systems

### 3.1 Polymers

Synthetic polymers can be ubiquitously found in daily-life commodities. From a basic point of view, since they do not easily crystallize, they can be considered as model systems to investigate the universal features of glass-forming systems, in particular the segmental dynamics in the glass-rubber transition zone. The main transition of amorphous polymers from glass to rubber softening dispersion usually involves different modes of molecular motion, including local segmental  $\alpha$  relaxation, sub-Rouse modes and Rouse modes [5]. The sub-Rouse modes were firstly found in polyisobutylene (PIB) by photon correlation spectroscopy and creep compliance measurements [6]. Recently, the sub-Rouse modes can be detected by dielectric spectroscopy in polyisoprene (PIP), head-to-head polypropylene (hhPP) and also in PIB [7]. The relaxation units of sub-Rouse modes involve backbone bonds on the order of 10, which are larger than the local segmental relaxation, but smaller than the Gaussian sub-molecules which is the basis unit of Rouse modes. The motion of the sub-Rouse modes is slower than local segmental motion due to longer length-scale of motion, but they are still faster than the Rouse modes. Well known are the facts that the Rouse modes are totally entropic and noncooperative, and the  $\alpha$  relaxation is cooperative [8]. However, the nature of the sub-Rouse modes is still not well understood.

Recently, a series of polymers such as polystyrene (PS), poly(methyl methacrylate) (PMMA), poly(vinyl acetate) (PVAc) have been measured by mechanical spectroscopy in torsion mode at a frequency range  $10^{-2}$ - $10^2$  Hz with a constant heating rate or at a given temperature versus frequency (isotherms) [9-13]. Fig. 2 displays the typical loss tangent isotherms of PS with  $M_w=2.7$  kg/mol at different temperatures above  $T_g$ . Due to the overlap and coupling of different molecular modes, it is difficult to resolve the contribution of each mode and gain more information. With the help of two-dimensional correlation analysis, three peaks are well resolved in the synchronous 2D correlation spectra of  $\tan \delta$  with frequency, corresponding to the  $\alpha$ -relaxation, the sub-Rouse mode and the Rouse mode, respectively [13]. For the sake of clarity, examples of the fits to the spectra at 402 K are given. From the fits, the relaxation times of the  $\alpha$ -relaxation, sub-Rouse modes and Rouse modes are obtained as a function of temperature. In Fig. 3 we plot the  $T$ -dependence of relaxation time  $\tau$  of the sub-Rouse modes for a typical example PMMA. A close examination of data reveals that the  $T$ -dependence of the sub-Rouse modes relaxation time cannot be described accurately by a single Vogel-Fulcher-Tammann (VFT) equation over the entire temperature range. Two VFT equations are required to fit the data of PMMA. This is confirmed by using the method proposed by Stickel and coworkers [14], whereby the data  $\tau(T)$  are transformed into  $\phi_T = (-d \log \tau / dT)^{-1/2}$  as a function of  $T$ . The crossover of  $\tau(T)$  from one VFT law to another is substantiated by  $\phi_T$  exhibiting a change in slope at some characteristic temperature  $T_B \sim 1.2 T_g$  (see the inset of Fig. 3).

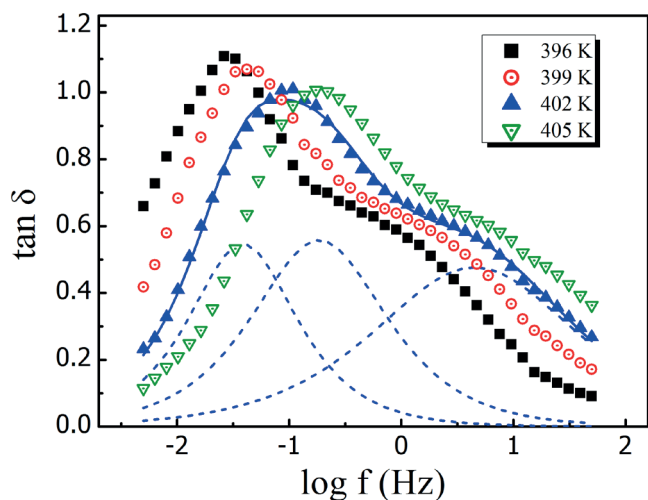


Fig. 2.  $\tan\delta$  versus frequency for PS with  $M_w=2.7$  kg/mol at 396, 399, 402 and 405 K. As an example, the  $\tan\delta$  spectrum at 402 K can be resolved into three peaks (dotted blue lines), corresponding to the local  $\alpha$  relaxation, sub-Rouse modes, and Rouse modes with decreasing frequency

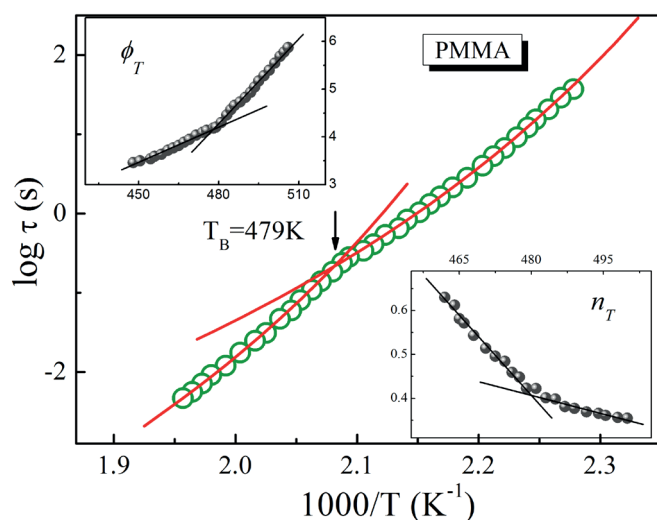


Fig. 3. The relaxation time  $\tau_{SR}$  of sub-Rouse modes versus  $1/T$  for PMMA with  $M_w=68$  kg/mol. The upper left inset shows the plots of the Stickel function,  $\phi_T = (-d\log(\tau_{SR}(T))/dT)^{-1/2}$ , against  $T$ . The lower right inset shows the  $T$ -dependence of coupling parameter  $n$  of sub-Rouse modes for the polymer

The only theoretical model for relating frequency dispersion to dynamics of relaxation processes is the coupling model (CM) [1,8,15], which identifies the broadening of the relaxation peak as being due to intermolecular coupling. In the CM, the broadening or degree of departure from exponential decay is measured by the coupling parameter,  $n$ , appearing in the exponent of the Kohlrausch–William–Watts function

$$\phi(t) = \exp[-(t/\tau)^{1-n}] \quad (2)$$

The coupling parameter  $n$  ( $0 \leq n < 1$ ) increases with increasing intermolecular interaction. The variation of  $n$  of the sub-Rouse modes for PMMA is presented in the inset of Fig. 3. As shown therein, on decreasing  $T$ ,  $n$  crosses over at  $T_B$  from slowly varying and small values of  $n$  to a more rapidly

increasing and larger values of  $n$ . The increase of  $n$  is usually monotonic, reaching the largest value at  $T_g$ . Therefore, the dynamic crossover of sub-Rouse modes, generally observed together with the  $\alpha$ -relaxation, is also a direct consequence of the marked increase in the intermolecular coupling below  $T_B$ , resulting in the onset of significant heterogeneity and non-exponentiality in the dynamics of the system.

Therefore, the sub-Rouse modes exhibit properties similar to those of local  $\alpha$ -relaxation. These similar properties indicate that the sub-Rouse modes, like the local  $\alpha$ -relaxation, are intermolecularly coupled and their dynamics are cooperative. Hence we conclude the existence of the sub-Rouse modes in the glass-rubber transition zone of amorphous polymers, as well as their properties and characteristics are universal. Furthermore, by invoking the results from the studies using positron annihilation spectroscopy and adiabatic calorimetry, we show both viscoelastic mechanisms of the  $\alpha$  relaxation and sub-Rouse modes are coupled to density, correlated with the change of the configuration entropy, and are intermolecularly cooperative, which is responsible for the reason why the sub-Rouse modes exhibit a similar crossover of dynamics at the same  $T_B$  as the  $\alpha$ -relaxation [16]. These findings enhance the understanding of the sub-Rouse modes and their manifestation in the viscoelasticity of polymers in the glass-rubber transition region.

### 3.2 Colloids

Understanding the mechanism of phase behaviors in colloidal systems is important in a broad range of science and technology. Generally, colloidal gels are arrested at low density where the particles are tightly bonded to each other. The leading mechanism for gelation is the attractive potentials between colloidal particles. Increasing concentration would result in a transition from a colloidal gel to an attractive glass. However, recent report indicates that the colloidal particles, such as microgels, exhibit at high concentration properties similar to that of a macroscopic gel [17]. In colloidal system with repulsive interactions, a glass-to-gel transition is observed with increasing concentration [18]. The simulation study also points out this transition [19]. Direct experimental evidences of the glass-to-gel transition and the common features of glasses and gels in colloids are still lacking. Further investigation is needed in order to gain a deeper understanding of this concentration-induced glass-to-gel transition.

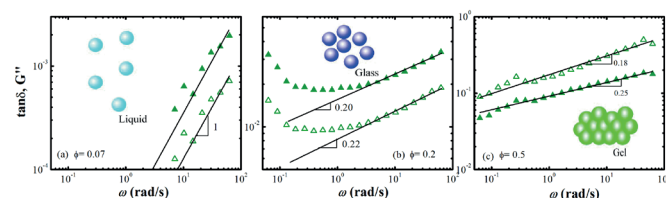


Fig. 4. Frequency dependences of  $G''$  (open symbols) and  $\tan\delta$  (solid symbols) for cross-link density = 6% PNIPAM microgel suspension at 25°C for three weight fractions: a) liquidlike state at 0.07; the solid lines show the expected low-frequency behavior of a viscoelastic liquid; b) glass state at 0.2; the power-law scaling fit lines for high frequency are plotted; c) gel state at 0.5; the solid lines show the frequency scaling behavior for a static percolated network. The cartoon illustration of PNIPAM microgels phase is shown in the relevant state.



Among most microgels, poly(*N*-isopropylacrylamide) (PNIPAM) microgels, with a lower critical solution temperature (LCST) of 33°C, have attracted considerable interests as model colloids, since the volume of them and the interaction between the microgels can be tuned precisely by temperature [20,21]. By using mechanical spectroscopy, the liquid, glass and gel transition in suspensions of PNIPAM microgel with three cross-link densities have been studied [22]. In Fig. 4, the loss modulus  $G''$  and loss tangent  $\tan\delta$  of PNIPAM microgel suspensions with a cross-link density of 6% are plotted as a function of frequency, in a log-log scale at  $T=25^\circ\text{C}$  and different weight fractions ( $\phi_w=0.07, 0.2, \text{ and } 0.5$ ). Depending on the weight fraction, three distinct behaviors are observed. At  $\phi_w=0.07$ , the frequency dependence of  $G''$  approaches the terminal behavior of a viscoelastic liquid,  $G'' \sim \omega^1$ , reflecting the liquid-like nature of the sample. Note that both  $G''$  and  $\tan\delta$  describe the energy dissipation behaviors of materials and so they exhibit a similar behavior in the whole frequency range. For  $\phi_w=0.2$ ,  $G''$  and  $\tan\delta$  show apparent minima, and the increase of  $G''$  and  $\tan\delta$  with decreasing  $\omega$  are supposed to be due to the additional energy dissipation induced by particles escaping from the cages formed by the neighboring particles. This indicates the presence of a structural relaxation at low frequencies that is a feature of glassy materials. At  $\phi_w=0.5$ , power-law scaling behaviors in  $G''$  and  $\tan\delta$  are observed in the whole frequency range that can be ascribed to the percolation transition since the power law relaxation spectrum implies the occurrence of the transient particle network.

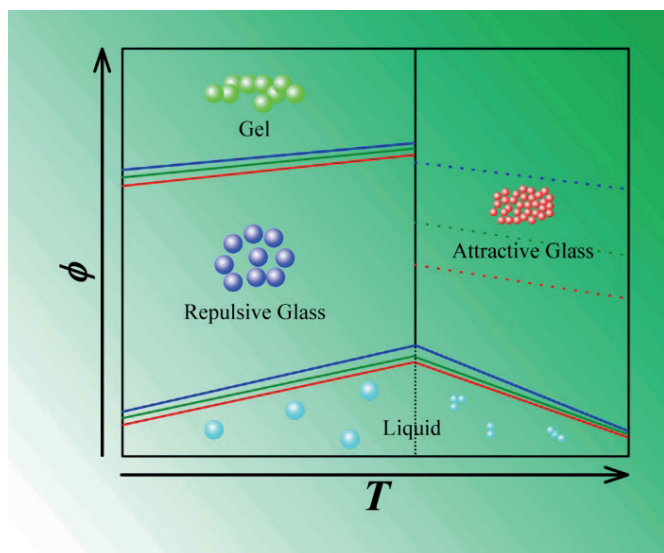


Fig. 5. Concentration and temperature dependent phase behavior of PNIPAM microgel suspensions controlled by different cross-link densities: 4% (lower red lines), 6% (middle olive lines) and 10% (upper blue lines). The dot color lines distinguish the significant glass feature with concentration in different crosslink densities

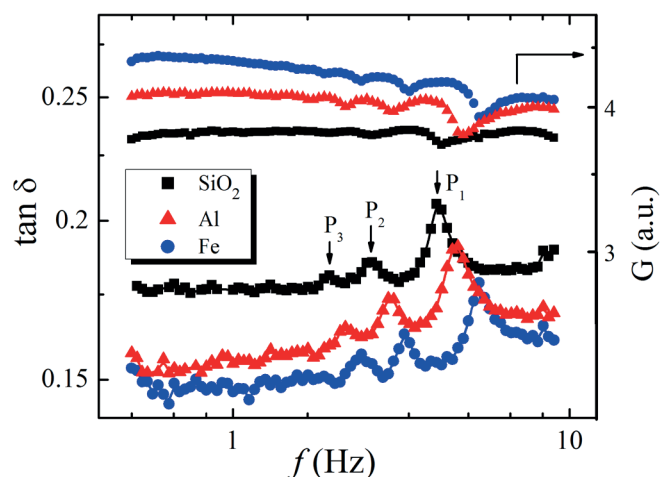


Fig. 6. Mechanical spectra ( $\tan\delta$  and  $G$ ) of fine sand, powdered Al and Fe as a function of frequency at the amplitude  $A_0=7.12 \times 10^{-6}$  m

Figure 5 shows the temperature and concentration controlled phase diagram of the PNIPAM microgels. Below the LCST, microgel suspension exhibits a liquid-like behavior. As concentration is increased, the motion of the particle is gradually restricted and at last microgel can only rattle within a cage formed by its neighboring particles, and so the system exhibits a glass phase. At this moderate concentration, the microgel particles exhibit repulsion due to the charge or steric stabilization. However, the situation is changed when the concentration is further increased, which leads to interpenetration of the outer and less-linked regions of the PNIPAM microgels as well as soft particles compression. As a result, the shape of particles starts to significantly deviate from the spherical one. This results in a favorite direction of the interaction between the particles, which in turn leads to the arising of branching events. Therefore, the cage structure is destroyed, finally leading to the percolation of the particles associated to a gel transition. It is worthwhile to mention that with increasing cross-link density, the overall trend of the glass and gel formation slightly shifts to higher concentrations. The possible reason is that the volume of the microgel particle decreases with increasing cross-link density.

Therefore, with increasing concentration the system undergoes a repulsive glass-to-gel transition below the LCST, while, as temperature is raised across the LCST, the system undergoes a gel-to-attractive glass transition. A mechanism of these transitions for the microgels is proposed based on the directional interaction between the particles. In moderate concentration or de-swelling microgels the interaction is isotropic leading to the glass phase, while in concentrated and deformed microgels the interaction is directional leading to the gel phase. The results enrich the current understanding of the phase transition in microgel systems and shed new light on the phase diagram of colloidal suspensions in general [22].

### 3.3 Granular matter

Granular materials are ubiquitous in nature, and they are widely used in the industry, from mining to agriculture, or in the pharmaceutical industry. The elastic properties of granular

systems receive much attention because they control numerous natural phenomena such as mudslides, avalanches, and debris flows. The contact force between two elastic spheres is known to obey the nonlinear Hertz law, which plays a key role in granular dynamics and energy dissipation. This model predicts that the speed of sound scales as  $1/6$  with the force  $F$  exerted on the particles. This relation has been observed in 1D granular systems but does not seem to be verified in higher dimensions because of geometrical effects [23]. To get rid of such problem, qualitative characterization of the relation of the grain contact force with the elastic modulus and deformation of grains is necessary and imperative in 3D actual granular systems, but it is hard to study by direct experimental investigation. The high-frequency acoustics has been usually adopted to uncover the elastic constants and dissipation mechanism of grain chains but it cannot provide any information about the grain structures on short length scales [24]. In contrast, the low-frequency dynamics of grain chains under a low vibration intensity  $\Gamma < 0.1$  has not received nearly as much attention, although the weakly excited granular media show a rich dynamic behavior and the multiple resonant dissipation peaks allow us to infer the length of the grain chain structure on short length scales [25].

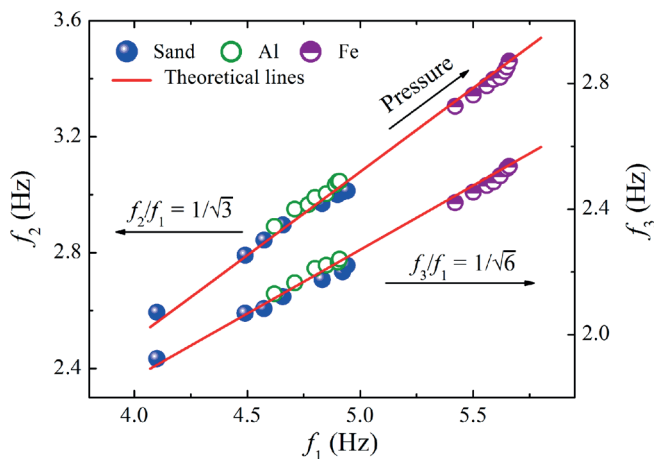


Fig. 7 Ratios of peak positions among  $f_1$ ,  $f_2$  and  $f_3$  for P1, P2 and P3 peaks with increasing pressure

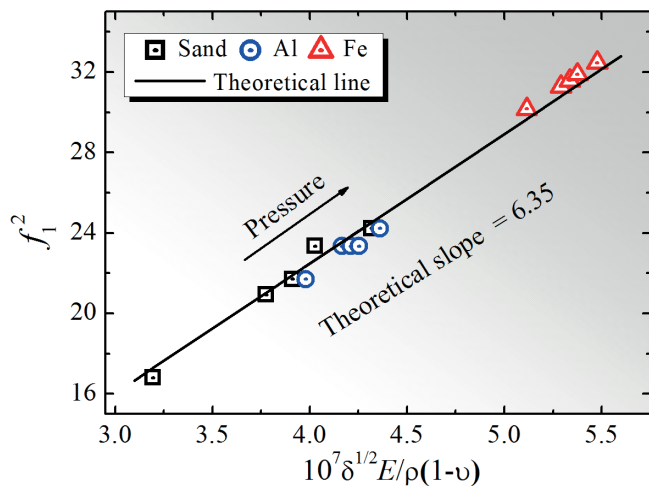


Fig. 8. Comparison of the model and experimental data in the resonance frequency of two grain chain as a function of  $\delta^{1/2}E/\rho(1-\nu)$  for different granular systems with increasing pressure

By using a force vibration method, we measured the dissipation spectra of granular systems made up of different kinds of grains [26]. Figure 6 is a typical frequency spectrum of energy dissipation and modulus of sand and powdered Al and Fe. For all types of granular systems, with decreasing frequency, three pronounced dissipation peaks, labeled as  $P_1$ ,  $P_2$ , and  $P_3$ , are detected in the frequency range of 0.5-9.0 Hz. Meanwhile, the modulus shows three corresponding minima. To define the origin of these peaks, we check their reproducibility and have not observed any obvious grain slip around the probe at the sample surface from visual observations. The dissipation peaks are independent of the surface roughness of the particles by measuring the dissipation spectra of glass beads with smooth surface but the same particle diameter to sand. So the dissipation peaks are assumed to result from the inherent resonant dissipation of grains chains with different lengths. As the frequency increases up to the resonant frequency of grain chains with a certain length, the blocked chains will be activated and become flexible. So the strength of the force chains will be softened. As a result, the resonance peak appears and the relative modulus exhibits a minimum.

Generally, the resonant frequency is inversely proportional to the length of the vibration system itself. In this sense, the dissipation peak  $P_1$  at higher frequency corresponds to the resonance of shortest chain, i.e., the two-particle force chain, while  $P_2$  and  $P_3$  corresponds to the resonance of three and four particle force chains, respectively. For a simple harmonic oscillation, the resonant frequency ( $f_{i-1}$ ) of grain chains made of  $i$  particles follows

$$f_{i-1} = \frac{1}{2\pi} \sqrt{\frac{k_i}{im}}, \quad i=2, 3, 4 \dots, \quad (3)$$

where  $m$  is the mass of a single particle,  $k_i$  is the stiffness coefficient of grain chain consisting of  $i$  particles. Assuming that the grain chain is linked by linear springs composed of two particles in series [23], the stiffness coefficient could be expressed by  $k_i = k_2/(i-1)$ , where  $k_2$  denotes the stiffness coefficient of the chain having two grains. According to Eq. (3), the ratios of resonant frequencies of grain chains with different lengths could be estimated. For instance, the ratio of

$f_1/f_2 = \sqrt{3}$  and  $f_1/f_3 = \sqrt{6}$ . In Fig. 7, we plot the ratios of peak positions among  $f_1$ ,  $f_2$  and  $f_3$  for P1, P2 and P3 peaks with increasing pressure. As shown, the ratios of  $f_2/f_1$  and  $f_3/f_1$  are constants, independent of the material properties of grain and pressure. Surprisingly, the experimental data of  $f_1/f_2$  and  $f_1/f_3$  agree well with the theoretical predictions. Thus these results give a solid confirmation that the loss peaks arise from the resonance dissipation of grain chains with different lengths.

The interaction between two adjacent particles is described by the nonlinear Hertz's law, and the relationship between the deformation  $\delta$  and the force  $F$  is given by

$$F = \frac{4}{3} R^2 \frac{E}{1-\nu} \delta^{\frac{3}{2}}, \quad (4)$$

where  $R$  is the radius of sphere,  $E$  is Young's modulus and  $\nu$  is Poisson's coefficient. This corresponds to a normal stiffness:

$$k = \frac{dF}{d\delta} = 2R^2 \frac{E}{1-\nu} \delta^{\frac{1}{2}}. \quad (5)$$

Combining Eq. (3) and (5), the resonant frequency  $f_1$  of two-particle force chain is written by

$$f_1^2 = \frac{R^2}{4\pi^2 \rho V} \frac{E}{1-\nu} \delta^{\frac{1}{2}}. \quad (6)$$

Based on Eq. (6),  $\delta$  can be quantified from the measured peak frequency  $f_1$  along with  $E$  and  $\nu$ . In Fig. 5, we show a master curve of the inherent frequency  $f_1$  of two-particle force chain and the deformation  $\delta$  for different granular systems. It can be found that with increasing pressure, the values of  $f_1^2$  increases linearly with  $\delta^{1/2}E/\rho(1-\nu)$ . The agreement between the experimental slope and the theoretical prediction ( $R^{1/2}/(4\pi^2V) = 6.35$ ) is striking. The above results suggest that the Hertz interaction fully accounts for the elasticity of grain chains under low-frequency weak excitation.

In addition, mechanical experiments for particles of different type and mass, and changing the experimental conditions such as immersed depth, applied amplitude and pressure all produce qualitatively similar results and illustrate the robustness of the phenomena [26]. Thus this is a strong experimental evidence of contact elasticity of grain chains in Hertz contact by investigating the low-frequency dissipation of short grain chains in elastic regime. This work provides a framework to characterize the properties of the grain chain under external pressure, and enables us to identify behaviors that are general across grain types [26].

#### 4. Conclusions

The last twenty years have witnessed rapid increasing research interest in the mechanical spectroscopy applications on soft matter. As one of the mechanical spectroscopy technique, the improved low-frequency inverted torsion pendulum with a Couette-like setup has become firmly established as a powerful and key tool to study many problems in soft matter area. Despite its potential, combination with other experimental techniques is usually required to gain deeper insight and nowadays such collaboration is becoming a common methodology. On the other hand, the advances in instrumentation will greatly enhance our ability to understand the dynamical behavior in soft matter systems, such as exploiting mechanical spectroscopy capabilities to explore systems with micro- and nanoscales. It can shed light into confinement effects on the local dynamics of nanostructured systems including polymers, colloids and biological systems.

#### Acknowledgment

This work was financially supported by National Natural Science Foundation of China (Grant No. 11174283 and 11374298).

#### REFERENCES

- [1] A.S. Nowick, B.S. Berry, *Anelastic Relaxation in Crystalline Solids*, Academic Press, New York, (1972).
- [2] F.Q. Zu, Z.G. Zhu, L.J. Guo, X.B. Qin, H. Yang, W.J. Shan, Observation of an anomalous discontinuous liquid-structure change with temperature, *Phys. Rev. Lett.* **89**, 125505 (2002).
- [3] R. Cantelli, The roots and the future of mechanical spectroscopy, *Mater. Sci. Eng. A* **442**, 5-20 (2006).
- [4] X.B. Wu, Q.L. Xu, J.P. Shui, Z.G. Zhu, Low-frequency mechanical spectroscopy study of conformational transition of polymer chains in concentrated solutions, *Rev. Sci. Instrum.* **79**, 126105 (2008).
- [5] K.L. Ngai, *Relaxation and Diffusion in Complex Systems*, Springer, New York, (2011).
- [6] D.J. Plazek, I.C. Chay, K.L. Ngai, C.M. Roland, Viscoelastic properties of polymers. 4. Thermorheological complexity of the softening dispersion in polyisobutylene, *Macromolecules* **28**, 6432-6436 (1995).
- [7] M. Paluch, S. Pawlus, A.P. Sokolov, K.L. Ngai, Sub-Rouse modes in polymers observed in dielectric spectroscopy, *Macromolecules* **43**, 3103-3106 (2010).
- [8] K.L. Ngai, D.J. Plazek, A.K. Rizos, Viscoelastic properties of amorphous polymers. 5. A coupling model analysis of the thermorheological complexity of polyisobutylene in the glass-rubber softening dispersion, *J. Polym. Sci., Part B: Polym. Phys.* **35**, 599-614 (1997).
- [9] X.B. Wu, X.M. Zhou, C.S. Liu, Z.G. Zhu, Slow dynamics of the  $\alpha$  and  $\alpha'$  relaxation processes in poly(methyl methacrylate) through the glass transition studied by mechanical spectroscopy, *J. Appl. Phys.* **106**, 013527 (2009).
- [10] X.B. Wu, Z.G. Zhu, Dynamic crossover of  $\alpha'$  relaxation in poly(vinyl acetate) above glass transition via mechanical spectroscopy, *J. Phys. Chem. B* **113**, 11147-11152 (2009).
- [11] X.B. Wu, H.G. Wang, C.S. Liu, Z.G. Zhu, Longer-scale segmental dynamics of amorphous poly(ethylene oxide)/poly(vinyl acetate) blends in the softening dispersion, *Soft Matter* **7**, 579-586 (2011).
- [12] X.B. Wu, C.S. Liu, Z.G. Zhu, K.L. Ngai, L.M. Wang, Nature of the sub-Rouse modes in the glass-rubber transition zone of amorphous polymers, *Macromolecules* **44**, 3605-3610 (2011).
- [13] X.B. Wu, H.G. Wang, Z.G. Zhu, C.S. Liu, Quantifying changes in the low-frequency dynamics of amorphous polymers by 2D correlation mechanical spectroscopy, *J. Phys. Chem. B* **117**, 467-472 (2013).
- [14] F. Stickel, E.W. Fischer, R. Richert, Dynamics of glass-forming liquids. I. Temperature-derivative analysis of dielectric relaxation data, *J. Chem. Phys.* **102**, 6251-6257 (1995).
- [15] S. Capaccioli, M. Paluch, D. Prevosto, L.M. Wang, K.L. Ngai, Many-body nature of relaxation processes in glass-forming systems, *J. Phys. Chem. Lett.* **3**, 735-743 (2012).
- [16] X.B. Wu, C.S. Liu, K.L. Ngai, Origin of the crossover in dynamics of the sub-Rouse modes at the same temperature as the structural  $\alpha$ -relaxation in polymers, *Soft Matter* **10**, 9324-9333 (2014).
- [17] F.D. Lorenzo, S. Seiffert, Macro- and microrheology of heterogeneous microgel packings, *Macromolecules* **46**, 1962-1972 (2013).
- [18] Z. Hu, X. Xia, Hydrogel nanoparticle dispersions with inverse thermoreversible gelation, *Adv. Mater.* **16**, 305-309 (2004).

- [19] J.C.F. Toledano, F. Sciortino, E. Zaccarelli, Colloidal systems with competing interactions: from an arrested repulsive cluster phase to a gel, *Soft Matter* **5**, 2390-2398 (2009).
- [20] B. Sierra-Martin, Y. Laporte, A.B. South, L.A. Lyon, A. Fernandez-Nieves, Bulk modulus of poly(N-isopropylacrylamide) microgels through the swelling transition, *Phys. Rev. E* **84**, 011406 (2011).
- [21] G. Romeo, A. Fernandez-Nieves, H.M. Wyss, D. Acerno, D.A. Weitz, Temperature- controlled transitions between glass, liquid, and gel states in dense p-NIPA suspensions, *Adv. Mater.* **22**, 3441-3445 (2010).
- [22] H.G. Wang, X.B. Wu, Z.G. Zhu, C.S. Liu, Z.X. Zhang, Revisit to phase diagram of poly(N-isopropylacrylamide) microgel suspensions by mechanical spectroscopy, *J. Chem. Phys.* **140**, 024908 (2014).
- [23] C. Coste, E. Falcon, S. Fauve, Solitary waves in a chain of beads under Hertz contact, *Phys. Rev. E* **56**, 6104-6117 (1997).
- [24] T. Brunet, X. Jia, P. Mills, Mechanisms for acoustic absorption in dry and weakly wet granular media, *Phys. Rev. Lett.* **101**, 138001 (2008).
- [25] P. Umbanhowar, M. van Hecke, Force dynamics in weakly vibrated granular packings, *Phys. Rev. E* **72**, 030301 (2005).
- [26] L.C. Chai, X.B. Wu, C.S. Liu, A universal scaling law of grain chain elasticity under pressure revealed by a simple force vibration method, *Soft Matter* **10**, 6614-6618 (2014).

*Received: 20 April 2015*

